Inorganic Chemistry

ARTICLE

pubs.acs.org/IC

Neptunium Thiophosphate Chemistry: Intermediate Behavior between Uranium and Plutonium

Geng Bang Jin,*[,†,‡] S. Skanthakumar,[‡] Richard G. Haire,[§] L. Soderholm,[‡] and James A. Ibers[†]

[†]Department of Chemistry, Northwestern University, Evanston, Illinois, 60208-3113, United States

[‡]Chemical Sciences and Engineering Division, Argonne National Laboratory, Argonne, Illinois 60439, United States

[§]Chemical Sciences Division, Oak Ridge National Laboratory, Oak Ridge, Tennessee 37831, United States

Supporting Information

ABSTRACT: Black crystals of $Np(PS_4)$, $Np(P_2S_6)_2$, $K_{11}Np_7(PS_4)_{13}$, and $Rb_{11}Np_7(PS_4)_{13}$ have been synthesized by the reactions of Np, P_2S_5, and S at 1173 and 973 K; Np, K_2S, P, and S at 773 K; and Np, Rb_2S_3, P, and S at 823 K, respectively. The structures of these compounds have been characterized by single-crystal X-ray diffraction methods. $Np(PS_4)$ adopts a three-dimensional structure with Np atoms coordinated to eight S atoms from four bidentate PS_4^{3-} ligands in a distorted square antiprismatic arrangement. $Np(PS_4)$ is isostructural to $Ln(PS_4)$ (Ln = La−Nd, Sm, Gd−Er). The structure of $Np(P_2S_6)_2$ is constructed from three interpenetrating diamond-type frameworks with Np atoms coordinated to eight S atoms from four bidentate $P_2S_6^{2-}$ ligands in a distorted square antiprismatic geometry. The centrosymmetric $P_2S_6^{2-}$ anion comprises two PS_2 groups connected by two bridging S centers. $Np(P_2S_6)_2$ is isostructural to $U(P_2S_6)_2$. $A_{11}Np_7(PS_4)_{13}$ (A = K, Rb) adopts a three-dimensional channel structure built from interlocking $[Np_7(PS_4)_{13}]^{11-}$-screw helices with A cations residing in the channels. The structure of $A_{11}Np_7(PS_4)_{13}$ includes four crystallographically independent Np atoms. Three are connected to eight S atoms in bicapped trigonal prisms. The other Np atom is connected to nine S atoms in a tricapped trigonal prism. $A_{11}Np_7(PS_4)_{13}$ is isostructural to $A_{11}U_7(PS_4)_{13}$. From Np−S bond distances and charge-balance, we infer that Np is trivalent in $Np(PS_4)$ and tetravalent in $Np(P_2S_6)_2$ and $A_{11}Np_7(PS_4)_{13}$. Np exhibits a behavior intermediate between U and Pu in its thiophosphate chemistry.

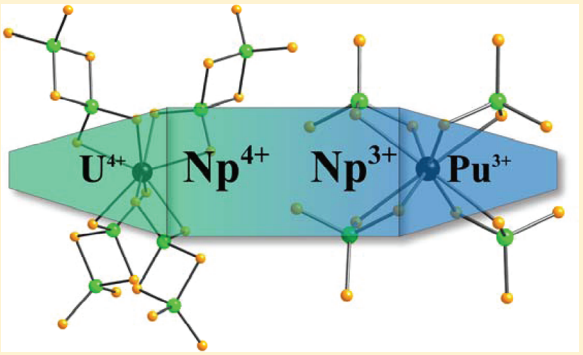

INTRODUCTION

Actinide elements and their compounds exhibit diverse chemical and physical properties owing to their accessible and partly filled 5f orbitals.[1] The 5f electrons show varying degrees of localization that range from itinerant band-like for light actinides to completely localized for elements Am and heavier. U, Np, and Pu are usually intermediate between these extremes.[2,3] For this reason, these lighter actinides are particularly interesting. U, Np, and Pu compounds display extremely rich chemistries with a number of stable oxidation states, even in the same compounds.[4−10] For example, the oxidation states of Np ions range from +3 to +7 in the redox window accessible in aqueous solutions.[11,12] In contrast, their chalcogenide chemistries have been much less explored, especially for Np and Pu.[7,10,13−19] In the known chalcogenide compounds, U is predominantly +4 with a few examples of +3 and +5.[13] Np exhibits stable +3 and +4 oxidation states in chalgogenides, within which some are isostructural to U analogues (e.g., $AMNpS_3$ (A = K, Rb, Cs; M = Cu, Ag)[14]) and the rest are isostructural to lanthanide analogues (e.g., $NpCuSe_2$[15]). Pu is predominantly +3 in chalcogenides with most compounds being isostructural to lanthanide analogues.[10,19]

Lanthanide (Ln) and actinide (An) oxophosphates have been extensively studied owing to their technological importance. These include the monazite class of minerals, $M(PO_4)$ (M = trivalent light lanthanides or actinides). Monazite is a promising host for the incorporation of actinide waste because of its potentially high actinide content, sintering capability, and stability under extreme conditions.[20−26] Although the chemistry of the oxophosphates and chalcophosphates differ because of their different redox properties and the weaker covalency of P−O bonds compared to P−Q (Q = S, Se) bonds, they have some comparative structural chemistry because of their similar anion geometries. A large number of actinide chalcophosphates, mainly of Th and U, have been synthesized during the past decade with the aid of reactive chalcophosphate fluxes.[27−37] Th and U chalcophosphates have shown an extremely rich structural chemistry resulting from a combination of various P_xQ_y anions and metals of high coordination numbers in diverse binding modes. Both Th and U exhibit a stable +4 oxidation state in structures that range from three-dimensional frameworks to isolated clusters. Four Pu chalcophosphates are known, namely $K_3Pu(PS_4)_2$ and $APu(P_2S_7)$ (A = K, Rb, Cs).[19] $K_3Pu(PS_4)_2$ is isostructural to $K_3Ln(PS_4)_2$ (Ln = Ce, La).[38,39] The structure of $APu(P_2S_7)$ is related

Received: July 13, 2011
Published: September 01, 2011

to that of $KSm(P_2S_7)$.[40] Thus, Pu thiophosphate chemistry is more lanthanide-like than that of Th or U. Remarkably, the chalcophosphate chemistry of Np, which lies between U and Pu, is unknown. Its position within the light actinide series provides an opportunity to examine structural systematics as the 5f orbitals fill and become more localized. Herein we present the syntheses and characterization of the first examples of Np thiophosphates: $Np(PS_4)$, $Np(P_2S_6)_2$, and $A_{11}Np_7(PS_4)_{13}$ (A = K, Rb).

EXPERIMENTAL SECTION

Syntheses. K (Cerac, 98%), Rb (Strem, 99%), P_2S_5 (Aldrich, 99%), P (Aldrich, 99%), and S (Mallinckrodt, 99.6%) were used as received. Brittle ^{237}Np chunks were crushed and used as provided (ORNL). K_2S and Rb_2S_3 were prepared by stoichiometric reactions of the elements in liquid NH_3.[41]

Caution! *^{237}Np is a α- and γ-emitting radioisotope and as such is considered a health risk. Its use requires appropriate infrastructure and personnel trained in the handling of radioactive materials. The procedures we use for the syntheses of Np compounds have been described.*[14]

For all the reactions, the reactants were loaded into fused-silica ampules in an Ar-filled glovebox and then flame-sealed under vacuum. The reaction mixtures were placed in a computer-controlled furnace and heated according to a specific temperature profile. The reaction products were washed with DMF and dried with acetone. Single crystals found in these reactions were used in the determination of their crystal structures.

$Np(PS_4)$. This compound was prepared through the reaction of Np (0.020 g, 0.084 mmol), P_2S_5 (0.019 g, 0.086 mmol), and S (0.003 g, 0.094 mmol). The reaction mixture was heated to 1173 K in 32 h, held at 1173 for 4 days, cooled to 773 K in 4.5 days, held at 773 for 2 days, and then cooled to 298 K in 6 h. The reaction products included large clusters of black irregular-shaped crystals of $Np(PS_4)$ and Np_3S_5[7] covered by a yellow powder. Only diffraction peaks from $Np(PS_4)$ and Np_3S_5 were found in the powder X-ray diffraction pattern of the product mixture. From the peak heights and areas, the yields of $Np(PS_4)$ and Np_3S_5 were roughly estimated to be 60% and 40%, respectively, based on Np.

$Np(P_2S_6)_2$. The same reaction mixture used for $Np(PS_4)$ was heated to 973 K in 20 h, held at 973 for 7.5 days, cooled to 673 K in 3.5 days, held at 673 for 10 h, and then cooled to 298 K in 5 h. The reaction products included large clusters of black irregular-shaped crystals of $Np(P_2S_6)_2$, $Np(PS_4)$, and Np_3S_5[7] covered by a yellow powder. Only diffraction peaks from $Np(P_2S_6)_2$, $Np(PS_4)$, and Np_3S_5 were found in the powder X-ray diffraction pattern of the reaction mixture. From the peak heights and area, the yields of $Np(P_2S_6)_2$, $Np(PS_4)$, and Np_3S_5 were roughly estimated to be 30%, 50%, and 20%, respectively, based on Np.

$K_{11}Np_7(PS_4)_{13}$. Black parallelepipeds of $K_{11}Np_7(PS_4)_{13}$ were obtained through the solid-state reaction of K_2S (0.014 g, 0.127 mmol), Np (0.019 g, 0.080 mmol), P (0.008 g, 0.258 mmol), and S (0.040 g, 1.25 mmol). The reactants were heated to 773 K in 16 h, held at 773 for 7 days, cooled to 373 K in 6 days, and then cooled to 298 K in 5 h. The products included many crystals of $K_{11}Np_7(PS_4)_{13}$ and unidentified black and yellow powders. The yield of $K_{11}Np_7(PS_4)_{13}$ was about 30% based on Np.

$Rb_{11}Np_7(PS_4)_{13}$. Black parallelepipeds of $Rb_{11}Np_7(PS_4)_{13}$ were obtained through the solid-state reaction of Rb_2S_3 (0.034 g, 0.127 mmol), Np (0.020 g, 0.080 mmol), P (0.008 g, 0.258 mmol), and S (0.032 g, 0.998 mmol). The reaction mixture was heated to 823 K in 16 h, held at 823 for 6 days, cooled to 423 K in 6 days, and then cooled to 298 K in 5 h. The products included many black crystals of $Rb_{11}Np_7(PS_4)_{13}$ and unidentified black and yellow powders. The yield of $Rb_{11}Np_7(PS_4)_{13}$ was about 20% based on Np.

Structure Determinations. Single-crystal X-ray diffraction data for $Np(PS_4)$ at 296 K and $Np(P_2S_6)_2$ and $A_{11}Np_7(PS_4)_{13}$ (A = K, Rb) at 100 K were collected with the use of graphite-monochromatized MoKα radiation (λ = 0.71073 Å) on a Bruker APEX2 diffractometer.[42] The crystal-to-detector distance was 5.106 cm. Data were collected by a scan of 0.3° in ω in groups of 606 frames at φ settings of 0°, 90°, 180°, and 270°. The exposure time was 10 s/frame for $Np(PS_4)$, 60 s/frame for $Np(P_2S_6)_2$, 20 s/frame for $K_{11}Np_7(PS_4)_{13}$, and 30 s/frame for $Rb_{11}Np_7(PS_4)_{13}$. The collection of intensity data as well as cell refinement and data reduction were carried out with the use of the program APEX2.[42] Face-indexed absorption corrections for $Np(PS_4)$ and $A_{11}Np_7(PS_4)_{13}$, and incident beam and decay corrections were performed with the use of the program SADABS.[43] The structures were solved with the direct-methods program SHELXS and refined with the least-squares program SHELXL.[44]

Table 1. Crystal Data and Structure Refinements for $Np(PS_4)$, $Np(P_2S_6)_2$, and $A_{11}Np_7(PS_4)_{13}$[a]

	$Np(PS_4)$	$Np(P_2S_6)_2$	$K_{11}Np_7(PS_4)_{13}$	$Rb_{11}Np_7(PS_4)_{13}$
Fw	396.21	745.60	4158.83	4668.90
space group	$I4_1/acd$	$I4_1/a$	$I\bar{4}2d$	$I\bar{4}2d$
Z	16	4	8	8
a, Å	10.8525(6)	12.832(3)	31.937(3)	32.063(1)
c, Å	19.249(1)	9.817(2)	17.269(2)	17.7798(8)
V, Å^3	2267.0(2)	1616.6(6)	17614(3)	18279(1)
T (K)	296(2)	100(2)	100(2)	100(2)
ρ_c, g/cm^3	4.643	3.063	3.137	3.393
μ, cm^{-1}	199.29	83.44	101.94	151.43
$R(F)$[b]	0.0219	0.0237	0.0376	0.0326
$R_w(F_o^2)$[c]	0.0822	0.0425	0.0864	0.0753

[a] For all structures, tetragonal system, λ = 0.71073 Å. [b] $R(F) = \Sigma||F_o| - |F_c||/\Sigma|F_o|$ for $F_o^2 > 2\sigma(F_o^2)$. [c] $R_w(F_o^2) = \{\Sigma[w(F_o^2 - F_c^2)^2]/\Sigma wF_o^4\}^{1/2}$ for all data. $w^{-1} = \sigma^2(F_o^2) + (qF_o^2)^2$ for $F_o^2 \geq 0$; $w^{-1} = \sigma^2(F_o^2)$ for $F_o^2 < 0$. q = 0.0198 for $Np(PS_4)$, 0.0123 for $Np(P_2S_6)_2$, 0.0120 for $K_{11}Np_7(PS_4)_{13}$, and 0.0278 for $Rb_{11}Np_7(PS_4)_{13}$.

The refinements of the structures of $Np(PS_4)$ and $Np(P_2S_6)_2$ were straightforward. The refinement of the structure of $A_{11}Np_7(PS_4)_{13}$ involved a model for the disorder of the A(7) cation. The program STRUCTURE TIDY[45] was used to standardize the positional parameters. Additional experimental details are given in Table 1 and in the Supporting Information.

Powder X-ray Diffraction. Powder X-ray diffraction patterns were collected with a Scintag X1 diffractometer with the use of Cu Kα radiation (λ = 1.5418 Å).

Bond Valence Sum Calculations. Bond valences, V,[46] were calculated from the formula $V = \Sigma_j \exp[(R_0 - R_j)/B]$, where the sum is over the j atoms in the first coordination sphere, R_j is the bond distance between the metal center and the jth atom, and R_0 and B are bond-valence parameters. The program Bond Valence Calculator, Version 2.0[47], was used with B = 0.37.

RESULTS

Syntheses. Owing to our limited quantity of Np metal and its radioactivity hazard, numerous uranium thiophosphate reactions were conducted before we explored the neptunium system. The compound $U(P_2S_6)$ $[U^{4+}(S_3P^{4+}{}_2S_3)]$[28] was prepared in almost 100% yield from a reaction of U, P_2S_5, and S in a molar ratio of 1:1:1 at 1173 K.[48] A similar reaction of Np to synthesize $Np(P_2S_6)_2$ failed. Instead, both $Np(PS_4)$ and Np_3S_5[7] were obtained. Several attempts to prepare pure $Np(PS_4)$ failed. For example, a stoichiometric reaction of Np, P_2S_5, and S at 1248 K resulted in a mixture of $Np(PS_4)$ and Np_3S_5.[7] Surprisingly, one of

dx.doi.org/10.1021/ic201493w |Inorg. Chem. 2011, 50, 9688–9695

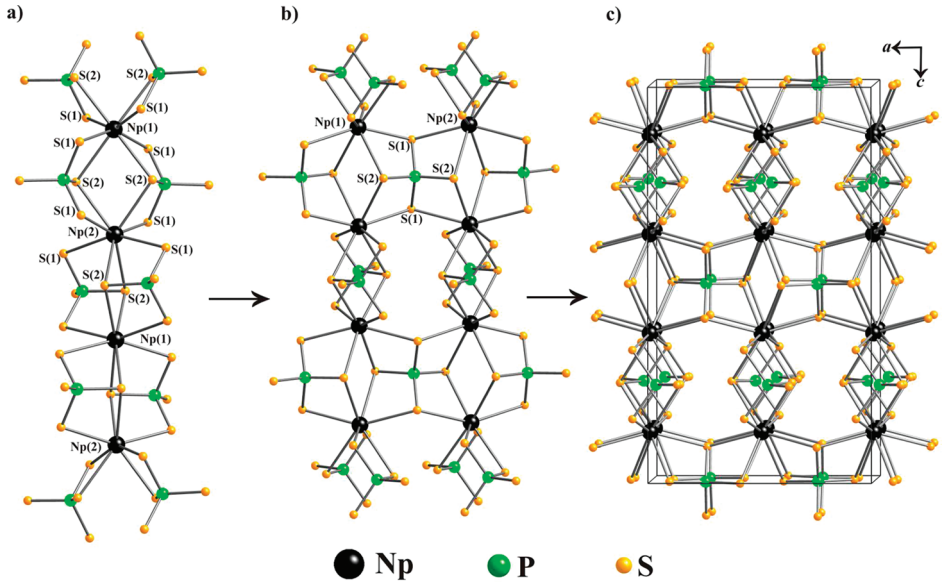

Figure 1. Crystal structure of $Np(PS_4)$. (a) Single edge-sharing NpS_8 polyhedral chain along the [001] direction; (b) Two single NpS_8 polyhedral chains sharing corners with each other between $Np(1)S_8$ and $Np(2)S_8$ polyhedral on the *ab* plane; (c) NpS_8 polyhedral chain connecting to four neighboring chains to form the three-dimensional structure of $Np(PS_4)$.

the failed reactions to prepare pure $Np(PS_4)$ that involved an excess of thiophosphate flux at 973 K produced $Np(P_2S_6)_2$ ($Np(S_2P^{5+}S_2P^{5+}S_2)_2$). Several variations in stoichiometries and temperature regimes did not improve the yield of $Np(P_2S_6)_2$. Reactions somewhat similar to those used to prepare several alkali-metal U or Pu thiophosphates around 773 K did afford modest yields of $A_{11}Np_7(PS_4)_{13}$, whereas the U analogues, $A_{11}U^{4+}{}_7(PS_4)_{13}$, were synthesized at 973 K.[36] Efforts made to prepare pure $A_{11}Np_7(PS_4)_{13}$ materials were not successful. $Np(PS_4)$, $Np(P_2S_6)_2$, $K_{11}Np_7(PS_4)_{13}$, and $Rb_{11}Np_7(PS_4)_{13}$ were obtained in yields of about 60%, 30%, 30%, and 20%, respectively.

From the many Np reactions that were carried out it is clear that the solid-state syntheses of Np thiophosphates diverge from those of the U thiophosphates. This is not surprising because the redox chemistry of the metals and their melting points (U: 1405.3 K; Np: 910 K) differ. The lower melting point of Np metal compared to U allows a relatively lower reaction temperature to be used to achieve a reasonable diffusion rate of reactants.

Structure of $Np(PS_4)$. $Np(PS_4)$ crystallizes in the $Pr(PS_4)$[49] structure type in space group $I4_1/acd$ of the tetragonal system. It is isostructural to $Ln(PS_4)$ (Ln = La−Nd, Sm, Gd−Er).[49] The structure of $Np(PS_4)$ includes two crystallographically unique Np positions (site symmetry of 222 for Np(1) and $\bar{4}$ for Np(2)) and one P position (site symmetry 2). Both Np centers are surrounded by eight S atoms from four bidentate tetrahedral PS_4^{3-} groups in a distorted square antiprismatic arrangement (Figure 1a), whereas each PS_4 tetrahedron shares an edge of S(1) and S(2) with two $Np(1)S_8$ and two $Np(2)S_8$ square antiprisms (Figure 1b). Each NpS_8 polyhedron shares an edge with two adjacent units in the fashion $-Np(1)S_8-Np(2)S_8-Np(1)S_8-Np(2)S_8-$ to form one-dimensional chains along [001] (Figure 1a). Furthermore, each NpS_8 polyhedral chain connects to four neighboring chains by sharing corners between $Np(1)S_8$ and $Np(2)S_8$ polyhedra in the *ab* plane to from a three-dimensional framework with open channels in all three directions (Figures 1b and 1c).

The related U compound $U_{0.75}(PS_4)$ is known.[33] It also possesses the $Pr(PS_4)$[49] structure type with the U(2) position being half occupied. In this structure type, there are no S−S bonds. Consequently, the formal oxidations states of +3, +5, −2 may be assigned to Np, P, and S in $Np(PS_4)$ and +4, +5, −2 to U, P, and S in $U_{0.75}(PS_4)$.[33]

Table 2. Selected Interatomic Distances (Å) for $Np(PS_4)$ and $Np(P_2S_6)_2$

$Np(PS_4)$		$Np(P_2S_6)_2$	
Np(1)−S(1) × 4	2.9309(5)	Np(1)−S(2) × 4	2.8579(8)
Np(1)−S(2) × 4	2.9702(5)	Np(1)−S(3) × 4	2.7997(9)
Np(2)−S(1) × 4	2.8839(5)	P(1)−S(1)[a]	2.107(1)
Np(2)−S(2) × 4	3.0419(5)	P(1)−S(1)[a]	2.115(1)
P(1)−S(1) × 2	2.0340(7)	P(1)−S(2)	1.990(1)
P(1)−S(2) × 2	2.0361(7)	P(1)−S(3)	1.996(1)
Np(1)···Np(2) × 2	4.8122(3)	Np(1)···Np(1) × 4	6.870(1)
Np(1)···Np(2) × 2	5.4262(3)	Np(1)···Np(1) × 4	9.766(1)

[a] Bridging atom.

Selected interatomic distances for $Np(PS_4)$ are listed in Table 2. All the Np−S and P−S distances are very close to the corresponding ones in $Nd(PS_4)$,[49] which is consistent with Np in the formal oxidation state +3. For example, the Np(1)−S distances are 2.9309(5) and 2.9702(5) Å vs Nd(1)−S distances of 2.934(2) and 2.971(2) Å; the Np(2)−S distances are 2.8839(5) and 3.0419(5) Å vs Nd(2)−S distances of 2.882(2) and 3.048(2) Å; and the P−S distances are 2.0340(7) and 2.0361(7) Å for Np vs 2.036(2) and 2.035(2) Å for Nd. Np−S distances are comparable to those found in Np_3S_5 for the eight-coordinate Np^{3+} cations, which are in the range of 2.8652(9)−3.024(1) Å.[7] The Np(1)···Np(2) distances between two edge-sharing NpS_8 polyhedra are 4.8122(3) Å, and the distances between two corner-sharing NpS_8 polyhedra are 5.4262(3) Å.

In $U_{0.75}(PS_4)$, U(1)−S distances are 2.863(2) and 2.895(2) Å, which are notably shorter than those of Np(1)−S.[33] If Np(1) and U(1) were in the same oxidation state, U(1)−S distances

dx.doi.org/10.1021/ic201493w |*Inorg. Chem.* 2011, 50, 9688–9695

would be expected to be about 0.02 Å longer than those of Np(1)−S because of the actinide contraction. In contrast, U(2)−S distances of 2.869(2) and 3.122(2) Å may be compared to Np(2)−S distances of 2.8839(5) and 3.0419(5) Å. This comparison is complicated because the U(2) position is only half occupied.

Structure of $Np(P_2S_6)_2$. $Np(P_2S_6)_2$ is isostructural to $U(P_2S_6)_2$ and crystallizes in the space group $I4_1/a$ of the tetragonal system.[32] The structure of $Np(P_2S_6)_2$ contains one crystallographically unique Np position (site symmetry $\bar{4}$) and one P and three S crystallographically unique atoms in general positions. As shown in Figure 2, each Np atom is surrounded by eight S atoms from four bidentate $P_2S_6^{2-}$ groups in a distorted square antiprism. The P_2S_6 moiety comprises S(2)S(3)P units bridged by S(1) atoms to give a centrosymmetric $P_2S_6^{2-}$ anion, which connects to two Np centers. Each resultant NpS_8 polyhedron connects to four other identical units to form adamantoid cages (Figure 3a). The structure of $Np(P_2S_6)_2$ consists of three interpenetrating adamantoid cage networks (Figure 3b). There are no S−S bonds in the structure of $Np(P_2S_6)_2$; the formal oxidation states of Np, P, S may be assigned as +4, +5, −2, respectively.

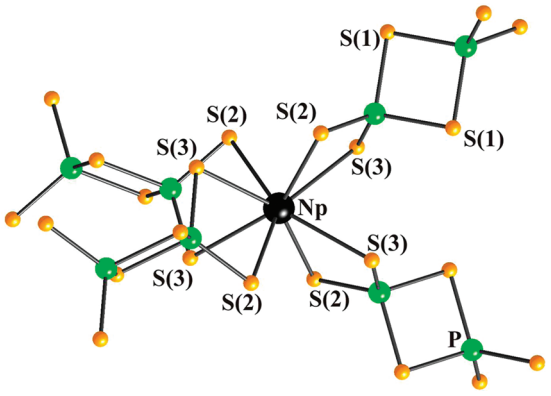

Figure 2. Coordination environment for the Np atom in $Np(P_2S_6)_2$.

Selected interatomic distances for $Np(P_2S_6)_2$ are presented in Table 2. Np−S distances are 2.8579(8) and 2.7997(9) Å, which are marginally shorter than the U−S distances of 2.879(1) and 2.812(1) Å in $U(P_2S_6)_2$, as expected.[32] These Np−S distances may be compared with other Np−S distances reported for Np^{4+} systems. For example, from 2.681(2) to 2.754(1) Å for six-coordinate Np^{4+} cations in $AMNpS_3$ (A = K, Rb, Cs; M = Cu, Ag) compounds,[14] from 2.6527(9) to 2.852(1) Å for the seven-coordinate Np^{4+} cations in $Np_3S_5^{7}$, and 2.889(2) and 2.9067(8) Å for nine-coordinate Np^{4+} cations in NpOS.[50] In $Np(P_2S_6)_2$, the P−S distances are 2.107(1) and 2.115(1) Å (bridging) and 1.990(1) and 1.996(1) Å (terminal), which are not statistically different from those of 2.107(2), 2.113(2), 1.989(2), and 1.997(2) Å in $U(P_2S_6)_2$.[32] The Np···Np distance between two metal centers bridged by a $P_2S_6^{2-}$ group is 9.766(1) Å within an adamantoid cage and the closest metal distance between two neighboring cages is 6.870(1) Å.

Structure of $A_{11}Np_7(PS_4)_{13}$ (A = K, Rb). $A_{11}Np_7(PS_4)_{13}$ is isostructural to $A_{11}U_7(PS_4)_{13}$.[36] The structure comprises seven crystallographically unique A, four Np, and seven P positions. Atoms Np(4), P(7), A(5), A(6), and A(7) have site symmetry 2, and the rest of the atoms are in general positions. Atoms Np(1), Np(3), and Np(4) are surrounded by eight S atoms from four bidentate tetrahedral PS_4^{3-} groups in bicapped trigonal prismatic arrangements, whereas each Np(2) atom is bound to nine S atoms from three bidentate and one tridentate tetrahedral PS_4^{3-} group in a tricapped trigonal prismatic geometry (Figure 4). Each $P(n)S_4$ (n = 1, 2, 3, 4, 6, 7) tetrahedron connects to two Np centers, whereas each $P(5)S_4$ unit connects to three Np atoms. Those NpS_x polyhedra connect to each other through bidentate PS_4^{3-} groups to form a $[Np_7(PS_4)_{13}]^{11-}$ helical chain that propagates along [001] (Figure 5). As shown in Figure 6, each $[Np_7(PS_4)_{13}]^{11-}$ chain further face and edge shares with

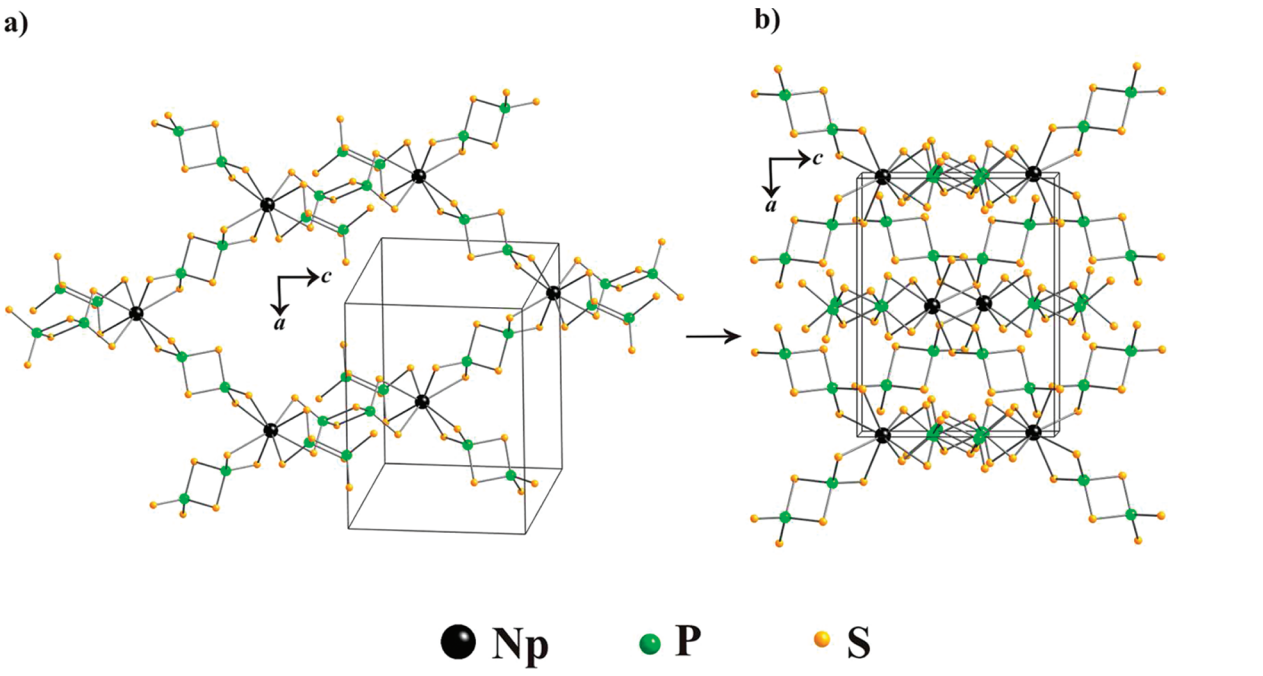

Figure 3. (a) Diamond-type framework in $Np(P_2S_6)_2$ constructed from adamantoid cages viewed down the [010] direction; (b) View of the three-dimensional structure of $Np(P_2S_6)_2$ down the [010] direction, which includes three interpenetrating diamond-type frameworks.

dx.doi.org/10.1021/ic201493w |Inorg. Chem. 2011, 50, 9688–9695

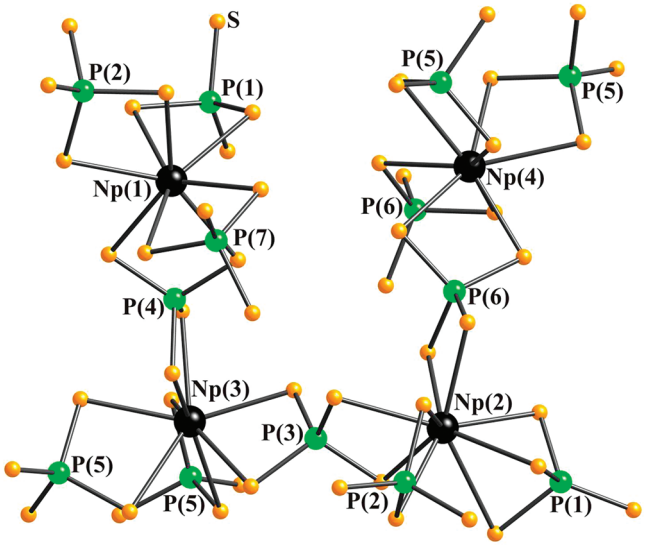

Figure 4. Coordination environments for four Np atoms and the connectivities between the neptunium sulfur polyhedra in $A_{11}Np_7(PS_4)_{13}$.

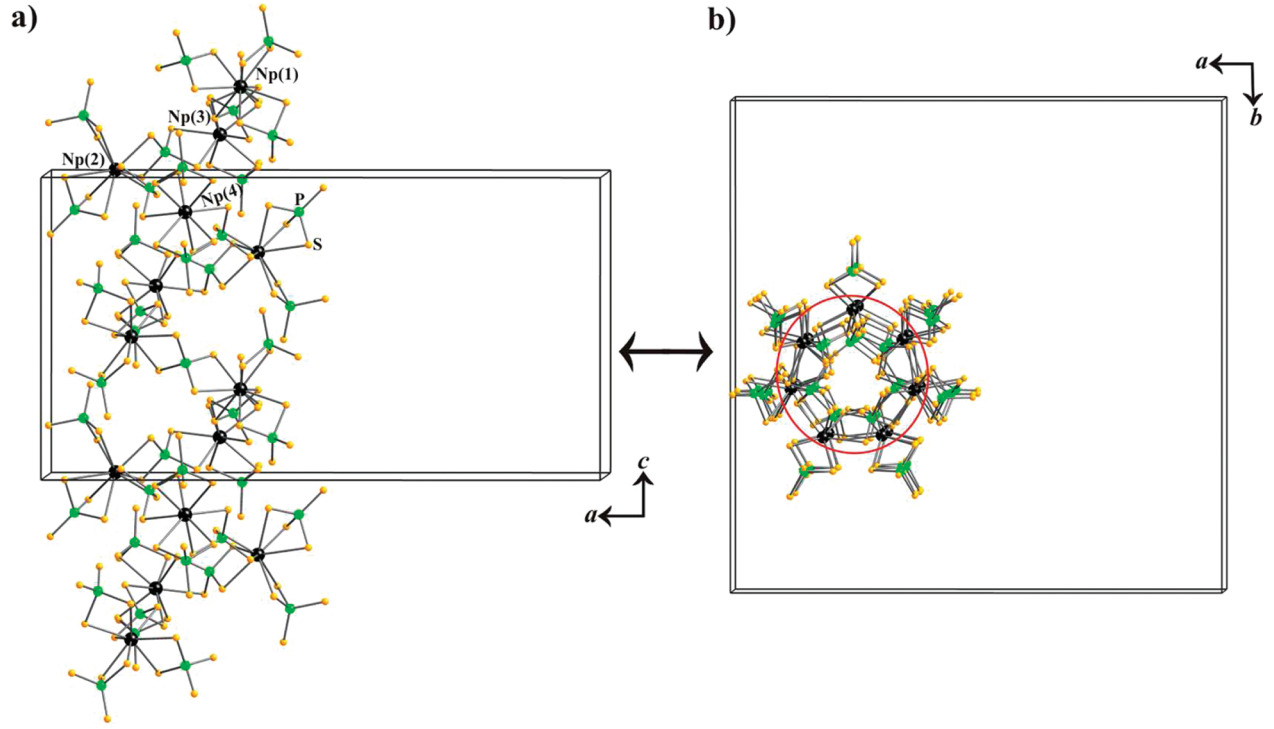

Figure 5. Single helical $[Np_7(PS_4)_{13}]^{11-}$ chain extending along the [001] direction in $A_{11}Np_7(PS_4)_{13}$: (a) view down the *b* axis ; (b) view down the *c* axis.

five neighboring chains on the *ab* plane to form a complex three-dimensional channel structure. The cavities created by $[Np_7(PS_4)_{13}]^{11-}$ chains are filled by the A atoms. There are no S−S bonds in the structure of $A_{11}Np_7(PS_4)_{13}$; charge balance is achieved with the formal oxidation states of A, Np, P, and S being assigned as +1, +4, +5, and −2, respectively.

Interatomic distances for $A_{11}Np_7(PS_4)_{13}$ may be found in the Supporting Information. Most of the Np−S and P−S distances for $K_{11}Np_7(PS_4)_{13}$ are within 0.01 Å of the corresponding ones in $Rb_{11}Np_7(PS_4)_{13}$. Only the distances for $K_{11}Np_7(PS_4)_{13}$ will be discussed. Np−S distances range from 2.722(3) to 2.915(3) Å for eight-coordinate Np atoms and from 2.805(3) to 3.109(3) Å for the nine-coordinate Np(2) atom. These are generally slightly shorter than the U−S distances in $K_{11}U_7(PS_4)_{13}$ because of the actinide contraction. The U−S distances range from 2.722(4) to 2.942(4) Å for eight-coordinate U atoms and from 2.821(4) to 3.110(5) Å for the nine-coordinate U cation.[36] Np−S distances for the eight-coordinate Np atoms are in the same range as those found in $Np(P_2S_6)_2$, and the values for the nine-coordinate Np atom are comparable to those found in NpOS.[50] Most are longer

dx.doi.org/10.1021/ic201493w |*Inorg. Chem.* 2011, 50, 9688–9695

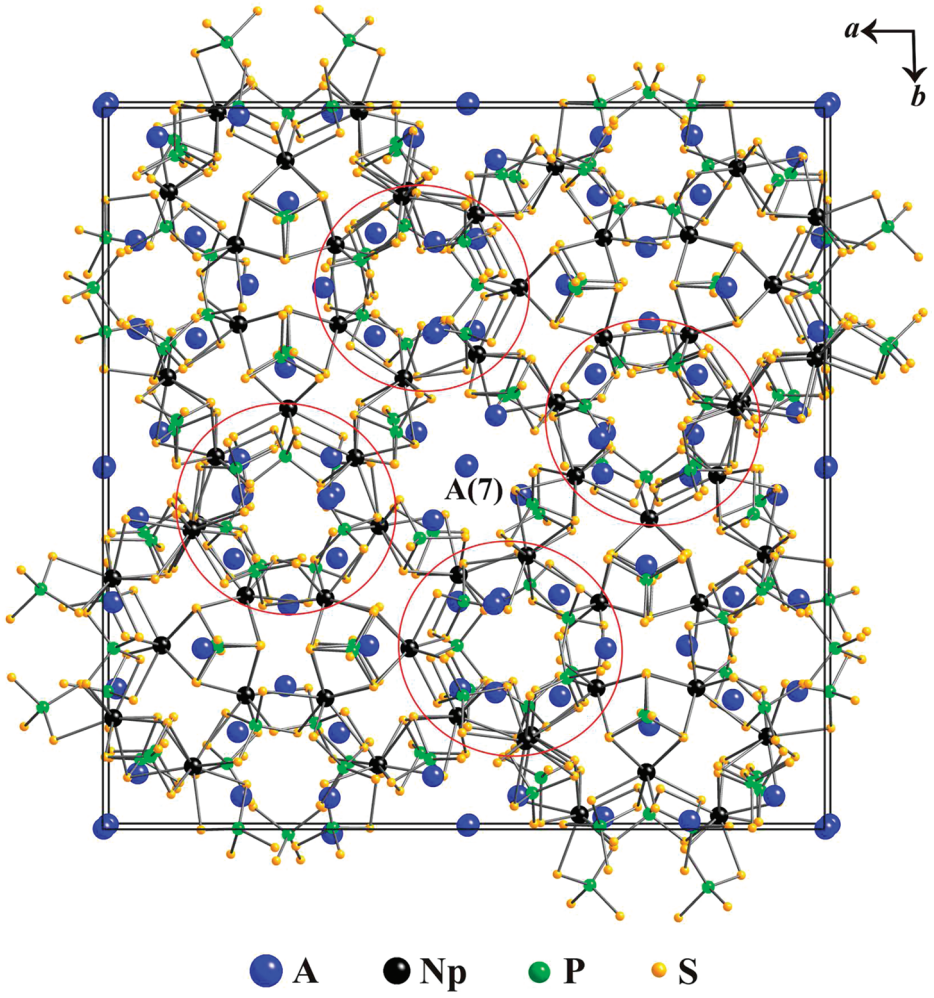

Figure 6. Each $[Np_7(PS_4)_{13}]^{11-}$ chain in $A_{11}Np_7(PS_4)_{13}$ shares faces and edges with five identical neighbors to form a three-dimensional channel structure, within which A^+ cations reside. $[Np_7(PS_4)_{13}]^{11-}$ chains are circled in red.

than those for the six-coordinate Np atoms in $AMNpS_3$ (A = K, Rb, Cs; M = Cu, Ag)[14] and the seven-coordinate Np atoms in Np_3S_5.[7] The P−S distances are in the range of 1.962(4) and 2.150(5) Å, close to those of 1.936(7) to 2.084(6) Å found in $K_{11}U_7(PS_4)_{13}$.[36] K−S and Rb−S distances are comparable to those found in $A_{11}U_7(PS_4)_{13}$.[36] The Np···Np distances between two neighboring metal centers bridged by a PS_4^{3-} anion within each helical chain are in the range of 6.906(1)−6.9778(8) Å. The Np(1)···Np(2) distances between two face-sharing neptunium sulfide polyhedra in neighboring helical chains are 4.1413(6) Å, and the distances between two edge-sharing NpS_8 polyhedra are 4.4219(8) Å for Np(3)···Np(3) and 4.3293(7) Å for Np(3)···Np(4).

Bond-Valence Analysis. Such an empirical analysis, when based on a multitude of literature data, provides an indication of the formal oxidation states of metal atoms in a given compound. However, there are too few Np−S distances available from single-crystal studies to make such an analysis meaningful. Instead, on the assumption that Np had a formal oxidation state of +4 in $AMNpS_3$ (A = K, Rb, Cs; M = Cu, Ag)[14] and +3/+4 in Np_3S_5[7], a value of the necessary bond-valence parameter R_0 of 2.56 was obtained from the Np−S distances in $AMNpS_3$ and Np_3S_5.[7] Similar calculations were performed for the present four compounds (Table 3) on the assumption that the formal oxidation states were +3 in $Np(PS_4)$ and +4 in $Np(P_2S_6)_2$, $K_{11}Np_7(PS_4)_{13}$, and $Rb_{11}Np_7(PS_4)_{13}$. The average value of R_0 is 2.57 for all ten compounds. The resulting valencies (Table 3) are reasonable.

DISCUSSION

The first four Np thiophosphates presented in the current study illustrate the divergence of Np thiophosphate chemistry from those of other early actindes. From single-crystal structural data and charge-balance considerations, Np cations are trivalent in $Np(PS_4)$ and tetravalent in $Np(P_2S_6)_2$ and $A_{11}Np_7(PS_4)_{13}$. With both stable +3 and +4 oxidation states, the thiophosphate chemistry of Np sits on the border between that of tetravalent U and trivalent Pu. Similar behaviors have been observed in their solution chemistry, which can be understood from a comparison of their relative An^{4+} standard reduction potentials ($E°$) in aqueous solutions under acidic conditions, −0.553(4) V for U, +0.22(1) V for Np, and +1.407(4) V for Pu.[51] Whereas these potentials are not expected to be reproduced in the solid-state sulfides discussed here, their trend often predicts redox stability in an isostructural series in which the lattice potentials and Fermi levels remain relatively constant.[52,53] From these potentials, it follows that among the three An^{3+} cations U^{3+} is the most susceptible to oxidation whereas Pu^{3+} is the least. In addition, the

dx.doi.org/10.1021/ic201493w |*Inorg. Chem.* 2011, 50, 9688–9695

Table 3. Bond-Valence Parameter R_0 and Bond Valence Sums

compound	atom	coordination number	assumed oxidation state[a]	derived R_0[b]	valence calculated from R_0 = 2.57
$Np(PS_4)$	Np(1)	8	+3	2.59	2.86
	Np(2)	8	+3	2.59	2.83
$Np(P_2S_6)_2$	Np(1)	8	+4	2.57	3.99
$K_{11}Np_7(PS_4)_{13}$	Np(1)	8	+4	2.55	4.24
	Np(2)	9	+4	2.57	3.97
	Np(3)	8	+4	2.56	4.15
	Np(4)	8	+4	2.56	4.12
$Rb_{11}Np_7(PS_4)_{13}$	Np(1)	8	+4	2.55	4.22
	Np(2)	9	+4	2.58	3.88
	Np(3)	8	+4	2.55	4.19
	Np(4)	8	+4	2.56	4.11

[a] From charge-balance considerations. [b] These values average to R_0 = 2.57. The average value of 2.57 resulted from incorporation of all derived R_0 values from $AMNpS_3$ (A = K, Rb, Cs; M = Cu, Ag),[14] Np_3S_5,[7] and the values above. This average value was used in a bond valence analysis to afford the tabulated valences.

reaction conditions, including the heating temperature and the presence of anions and other cations, can also affect the oxidation state of the final product. $Np^{3+}(PS_4)^{3-}$ was synthesized at a temperature 200 K higher than that of $Np^{4+}(P_2S_6)^{2-}{}_2$, presumably beyond the temperature necessary to decompose $P_2S_6^{2-}$ anions to PS_4^{3-} anions. It is not surprising that the PS_4^{3-} anions attract the trivalent Np cations, while two $P_2S_6^{2-}$ anions favor one tetravalent cation to form stable compounds. For the reactions of $A_{11}Np_7(PS_4)_{13}$, electropositive A^+ cations may help to stabilize the higher valence of Np, Np^{4+}, owing to the inductive effect.[54] The structural chemistry of Np thiophosphates is expected to be a combination of those of U^{4+} or Th^{4+} and Ln^{3+}, which is well exemplified here, with $Np(PS_4)$ isostructural to lanthanide analogues and $Np(P_2S_6)_2$ and $A_{11}Np_7(PS_4)_{13}$ isostructural to uranium analogues. In addition, compared to lanthanides and other lighter actinides, it is more likely for Np compounds to adopt new structure types containing both trivalent and tetravalent metal sites, as demonstrated by the mixed-valence binary compound, $(Np^{3+})_2Np^{4+}S_5$[7] found under those reaction conditions.

As noted in the Introduction, monazite ($M(PO_4)$ (M = trivalent light lanthanides or actinides) has been studied for use as a solid-state matrix in a spent nuclear fuel repository. It is interesting to compare the structure of $M(PS_4)$ with that of monazite. Similar to $M(PS_4)$, the monazite structure contains interconnecting arrangements of metal polyhedral chains; however, each chain shares metal polyhedral edges with six neighboring chains to form a three-dimensional network without open channels.[22] The metal polyhedra in monazite are much more close packed than those in $M(PS_4)$. For example, the calculated densities from the X-ray structural data for $Gd(PO_4)$[22] and $Gd(PS_4)$[49] are 6.00 and 3.83 g/cm^3, respectively. This large structural deviation of $M(PS_4)$ from that of $Ln(PO_4)$ arises, at least in part, because there is less steric repulsion between the metal and P atoms for thiophosphates than for oxophosphates. For example, the Dy···P distance between edge-sharing DyS_8 and PS_4 polyhedra in $Dy(PS_4)$[49] is 3.591 Å, whereas the Dy···P distance between edge-sharing DyO_8 and PO_4 polyhedra in $Dy(PO_4)$[22] is 3.019 Å. As a result, PS_4^{3-} anions most commonly ligate large metal cations in multidentate modes, as shown here and in other actinide thiophosphates.[19,27,33,35−37] In contrast, PO_4^{3-} anions more commonly bind large metal cations in a monodentate mode, as found in low valent actinide phosphates.[55] In the structure of $M(PS_4)$, each metal center connects to four bidentate tetrahedral PS_4^{3-} groups, whereas the metal cation in the monazite structure is coordinated by nine O atoms from seven PO_4^{3-} groups, two of which are bidentate and the other five are monodentate.[22] Clearly each metal center in the monazite structure binds to more ligands, which gives rise to a more dense structure than that of $M(PS_4)$. One of the merits monazite has as a potential waste form for actinides is that it can accommodate most of the actinides without affecting the phase homogeneity. Trivalent actinide (U, Pu, Am−Bk) cations can readily replace the lanthanide cation because they have the same charge and similar radii. However, for substitution of the lanthanide by tetravalent actinides (Th, U, Np, Pu), charge balance has to be achieved by substitution mechanisms that involve the use of divalent cations such as Ca^{2+} or the SiO_4^{4-} anion.[25,26] The orthothiophosphate structure type, because it can accommodate Ln^{3+}, Np^{3+}, as well as U^{4+}cations, is potentially superior to monazite as a waste form in this regard. Future research directions include syntheses and structural characterization of Th, Pu, and mixed lanthanide actinide orthothiophosphates as well as measurements of their electronic and magnetic properties.

CONCLUSIONS

$Np(PS_4)$ is found to be isostructural to lanthanide analogues, whereas $Np(P_2S_6)_2$ and $A_{11}Np_7(PS_4)_{13}$ are shown to be isostructural to uranium analogues. Not only the charge-balance considerations but also comparisons of metric data indicate that Np is trivalent in $Np(PS_4)$ and tetravalent in $Np(P_2S_6)_2$ and $A_{11}Np_7(PS_4)_{13}$. Thus, Np exhibits a behavior intermediate between U and Pu in thiophosphate chemistry. In addition, the present results have led to an improved bond-valence parameter R_0 for Np and to a better understanding of the change in Np−Q bond distances with oxidation states.

ASSOCIATED CONTENT

Supporting Information. Crystallographic files in cif format for $Np(PS_4)$, $Np(P_2S_6)_2$, $K_{11}Np_7(PS_4)_{13}$, and $Rb_{11}Np_7(PS_4)_{13}$. This material is available free of charge via the Internet at http://pubs.acs.org.

AUTHOR INFORMATION

Corresponding Author
*E-mail: gjin@anl.gov.

ACKNOWLEDGMENT

The research was supported at Northwestern University by the U.S. Department of Energy, Basic Energy Sciences, Chemical Sciences, Biosciences, and Geosciences Division and Division of Materials Sciences and Engineering Grant ER-15522 and at Argonne National Laboratory under contract DEAC02-06CH11357.

REFERENCES

(1) Morss, L. R.; Edelstein, N. M.; Fuger, J., Eds. *The Chemistry of the Actinide and Transactinide Elements*, Third ed.; Springer: Dordrecht, 2006.

(2) Petit, L.; Svane, A.; Szotek, Z.; Temmerman, W. M.; Stocks, G. M. *Phys. Rev. B* **2010**, *81*, 045108.

(3) Denning, R. G. *J. Phys. Chem. A* **2007**, *111*, 4125–4143.

(4) Potel, M.; Brochu, R.; Padiou, J.; Grandjean, D. *C. R. Seances Acad. Sci., Ser. C* **1972**, *275*, 1419–1421.

(5) Loopstra, B. O. *Acta Crystallogr., Sect. B* **1970**, *26*, 656–657.

(6) Almond, P. M.; Sykora, R. E.; Skanthakumar, S.; Soderholm, L.; Albrecht-Schmitt, T. E. *Inorg. Chem.* **2004**, *43*, 958–963.

(7) Jin, G. B.; Skanthakumar, S.; Haire, R. G.; Soderholm, L.; Ibers, J. A. *Inorg. Chem.* **2011**, *50*, 1084–1088.

(8) Wang, S.; Alekseev, E. V.; Ling, J.; Skanthakumar, S.; Soderholm, L.; Depmeier, W.; Albrecht-Schmitt, T. E. *Angew. Chem., Int. Ed.* **2010**, *49*, 1263–1266.

(9) Haschke, J. M.; Allen, T. H.; Morales, L. A. *Science* **2000**, *287*, 285–287.

(10) Clark, D. L.; Hecker, S. S.; Jarvinen, G. D.; Neu, M. P., Plutonium. In *The Chemistry of the Actinide and Transactinide Elements*, Third ed.; Morss, L. R.; Edelstein, N. M.; Fuger, J., Eds.; Springer: Dordrecht, 2006; Vol. 2, pp 813−1264.

(11) Antonio, M. R.; Soderholm, L.; Williams, C. W.; Blaudeau, J.-P.; Bursten, B. E. *Radiochim. Acta* **2001**, *89*, 17–25.

(12) Williams, C. W.; Blaudeau, J.-P.; Sullivan, J. C.; Antonio, M. R.; Bursten, B.; Soderholm, L. *J. Am. Chem. Soc.* **2001**, *123*, 4346–4347.

(13) Narducci, A. A.; Ibers, J. A. *Chem. Mater.* **1998**, *10*, 2811–2823.

(14) Wells, D. M.; Jin, G. B.; Skanthakumar, S.; Haire, R. G.; Soderholm, L.; Ibers, J. A. *Inorg. Chem.* **2009**, *48*, 11513–11517.

(15) Wells, D. M.; Skanthakumar, S.; Soderholm, L.; Ibers, J. A. *Acta Cryst., Sect. E* **2009**, *65*, i14.

(16) Thévenin, T.; Jové, J.; Pagès, M. *Hyperfine Interact.* **1984**, *20*, 173–186.

(17) Thévenin, T.; Pagès, M.; Wojakowski, A. *J. Less-Common Met.* **1982**, *84*, 133–137.

(18) Charvillat, J. P.; Wojakowski, A.; Damien, D. *Proceedings of the 2nd International Conference on the Electron Structure of Actinides*, 1977; pp 469−473. (Ossolineum, Wrocław, Poland, 1976).

(19) Hess, R. H.; Gordon, P. L.; Tait, C. D.; Abney, K. D.; Dorhout, P. K. *J. Am. Chem. Soc.* **2002**, *124*, 1327–1333.

(20) McCarthy, G. J.; White, W. B.; Pfoertsch, D. E. *Mater. Res. Bull.* **1978**, *13*, 1239–1245.

(21) Mullica, D. F.; Grossie, D. A.; Boatner, L. A. *J. Solid State Chem.* **1985**, *58*, 71–77.

(22) Ni, Y.; Hughes, J. M.; Mariano, A. N. *Am. Mineral.* **1995**, *80*, 21–26.

(23) Meldrum, A.; Boatner, L. A.; Weber, W. J.; Ewing, R. C. *Geochim. Cosmochim. Acta* **1998**, *62*, 2509–2520.

(24) Kitaev, D. B.; Volkov, Y. F.; Orlova, A. I. *Radiochemistry* **2004**, *46*, 211–217.

(25) Bregiroux, D.; Terra, O.; Audubert, F.; Dacheux, N.; Serin, V.; Podor, R.; Bernache-Assollant, D. *Inorg. Chem.* **2007**, *46*, 10372–10382.

(26) Jardin, R.; Pavel, C. C.; Raison, P. E.; Bouëxière, D.; Santa-Cruz, H.; Konings, R. J. M.; Popa, K. *J. Nucl. Mater.* **2008**, *378*, 167–171.

(27) Simon, A.; Peters, K.; Peters, E.-M.; Hahn, H. *Z. Anorg. Allg. Chem.* **1982**, *491*, 295–300.

(28) Do, J.; Kim, J.; Lah, S.; Yun, H. *Bull. Korean Chem. Soc.* **1993**, *14*, 678–681.

(29) Chrondroudi, K.; Kanatzidis, M. G. *C. R. Acad. Sci. Paris* **1996**, *322* (Ser IIb), 887–894.

(30) Chrondroudi, K.; Kanatzidis, M. G. *J. Am. Chem. Soc.* **1997**, *119*, 2574–2575.

(31) Briggs Piccoli, P. M.; Abney, K. D.; Schoonover, J. R.; Dorhout, P. K. *Inorg. Chem.* **2000**, *39*, 2970–2976.

(32) Gieck, C.; Rocker, F.; Ksenofontov, V.; Gütlich, P.; Tremel, W. *Angew. Chem., Int. Ed. Engl.* **2001**, *40*, 908–911.

(33) Gieck, C. Ph.D. Dissertation, Johannes-Gutenberg Universität: Mainz, 2003.

(34) Briggs Piccoli, P. M.; Abney, K. D.; Schoonover, J. D.; Dorhout, P. K. *Inorg. Chem.* **2001**, *40*, 4871–4875.

(35) Hess, R. F.; Abney, K. D.; Burris, J. L.; Hochheimer, H. D.; Dorhout, P. K. *Inorg. Chem.* **2001**, *40*, 2851–2859.

(36) Gieck, C.; Tremel, W. *Chem.—Eur. J.* **2002**, *8*, 2980–2987.

(37) Chan, B. C.; Hess, R. F.; Feng, P. L.; Abney, K. D.; Dorhout, P. K. *Inorg. Chem.* **2005**, *44*, 2106–2113.

(38) Gauthier, G.; Jobic, S.; Brec, R.; Rouxel, J. *Inorg. Chem.* **1998**, *37*, 2332–2333.

(39) Evenson, C. R., IV; Dorhout, P. K. *Inorg. Chem.* **2001**, *40*, 2884–2891.

(40) Goh, E.-Y.; Kim, E.-J.; Kim, S.-J. *J. Solid State Chem.* **2001**, *160*, 195–204.

(41) Sunshine, S. A.; Kang, D.; Ibers, J. A. *J. Am. Chem. Soc.* **1987**, *109*, 6202–6204.

(42) *APEX2*, version 2009.5-1; *SAINT*, version 7.34a; Bruker Analytical X-Ray Instruments, Inc.: Madison, WI, 2009.

(43) *SMART*, version 5.054; *SAINT-Plus*, version 6.45a; Bruker Analytical X-Ray Instruments, Inc.: Madison, WI, 2003.

(44) Sheldrick, G. M. *Acta Crystallogr., Sect. A* **2008**, *64*, 112–122.

(45) Gelato, L. M.; Parthé, E. *J. Appl. Crystallogr.* **1987**, *20*, 139–143.

(46) Brown, I. D.; Altermatt, D. *Acta Crystallogr., Sect. B* **1985**, *41*, 244–247.

(47) Hormillosa, C.; Healy, S.; Stephen, T. *Bond Valence Calculator*, V2.0, McMaster University: Canada, 1993.

(48) Jin, G. B.; Ibers, J. A. Unpublished results.

(49) Komm, T.; Gudat, D.; Schleid, T. *Z. Natur. B: Chem. Sci.* **2006**, *61*, 766–774.

(50) Jin, G. B.; Raw, A. D.; Skanthakumar, S.; Haire, R. G.; Soderholm, L.; Ibers, J. A. *J. Solid State Chem.* **2010**, *183*, 547–550.

(51) Konings, R. J. M.; Morss, L. R.; Fuger, J., Thermodynamic Properties of Actinides and Actinide Compounds. In *The Chemistry of the Actinide and Transactinide Elements*, Third ed.; Morss, L. R.; Edelstein, N. M.; Fuger, J., Eds.; Springer: Dordrecht, The Netherlands, 2006; Vol. 4, pp 2113−2224.

(52) Soderholm, L.; Williams, C.; Skanthakumar, S.; Antonio, M. R.; Conradson, S. *Z. Phys. B.* **1996**, *101*, 539–545.

(53) Chiang, M.-H.; Antonio, M. R.; Williams, C. W.; Soderholm, L. *Dalton Trans.* **2004**, 801–806.

(54) Etourneau, J.; Portier, J.; Ménil, F. *J. Alloys Compd.* **1992**, *188*, 1–7.

(55) Orlova, A. I., Chemistry and Structure Chemistry of Anhydrous Tri- and Tetravalent Actinide Orthophosphates. In *Structural Chemistry of Inorganic Actinide Compounds*; Krivovichev, S. V.; Burns, P. C.; Tananaev, I. G., Eds.; Elsevier: Amsterdam, 2007; pp 315−340.